Quantum Chemical Calculations and Experimental Evidence for O-Bonding of Carbon Monoxide to Alkali Metal Cations in Zeolites

P. Ugliengo, E. Garrone,* A. M. Ferrari, and A. Zecchina

Dipartimento di Chimica IFM, Universitá di Torino, Via P. Giuria 7, 10125 Torino, Italy

C. Otero Areán

Departamento de Quimica, Universidad de las Islas Baleares, 07071 Palma de Mallorca, Spain

Received: May 1, 1999; In Final Form: April 1, 1999

By the comparison of experimental results and computational data concerning the interaction of CO with one or two naked cations, evidence is provided that weak bands occurring in the IR spectra of basic zeolites, after the low-temperature adsorption of CO, at frequencies lower than that of the gaseous molecule, are due to species O-bonded to a single cation in thermodynamic equilibrium with the usual, more stable species C-bonded to the same cation. The absence of O-bonding for CO in other systems is discussed, and evidence is provided for the probable occurrence in protonic zeolites.

1. Introduction

Carbon monoxide adsorbed on alkali metal exchanged zeolites has long been known to show as a minor feature in the IR spectra, a weak band at a frequency lower than 2143 cm^{-1} (the gas-phase value of ν(CO)). Seanor and Amberg, who first reported this finding, ascribed it to CO molecules somehow in "interaction with the lattice".[1] The location of such a band, however, does depend on the nature of the cation, in particular when comparing alkali-exchanged with Zn^{2+}- or Ca^{2+}-exchanged zeolites.[2]

Indeed, it is not straighforward to propose an explanation, because ν(CO) values lower than 2143 cm^{-1} are usually only accounted for by the interaction of CO with transition metal centers. When carbon monoxide binds to non-d cations in basic zeolites, electrostatic considerations suffice to describe the main features of the interaction.[3−7] Because coordination through the C end increases ν(CO), a way to explain a bathochromic shift of ν(CO) is to assume coordination through the O end. However, taking into account that on other systems (and in particular on metal oxides and halides) coordination of CO through the O end has never been documented, such a proposal cannot be made lightheartedly. Some of us, in a study devoted to the adsorption of CO on alkali cation exchanged ZSM-5 zeolites, have proposed that low-frequency bands are due to a double coordination of CO through both ends to suitably spaced cations.[2,8] Katoh et al.[9] have proposed instead that C-end and O-end coordination may occur simultaneously on the same cation.

We have recently studied[6] the whole set of CO adducts with naked alkaline cations (Li^+, Na^+, K^+, Rb^+, Cs^+) both in the X^+−CO and X^+−OC configuration (referred to hereafter as C-bonded and O-bonded, respectively), by means of several ab initio techniques. The results obtained indicate that coordination through the C end is always more energetic; when going from Li^+ to Cs^+, however, the difference in interaction energy decreases substantially. This fact may allow the simultaneous formation of C-bonded and O-bonded adducts on the same cation, as an effect of the equilibrium between the two modes of CO bonding to the same cation. Such a possibility is implicit in the paper by Katoh et al.,[9] but not explicitly discussed.

SCHEME 1

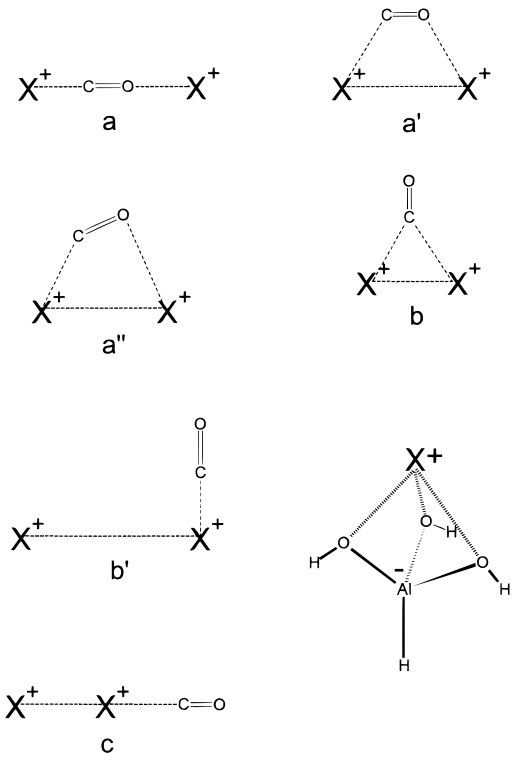

Recently, similar calculations as in our previous work have been performed considering, instead of the naked cations, cluster models (like $HAl(OH)_3^-X^+$) mimicking, in some way, the alkaline cations in the zeolitic matrix[10] (hereafter referred to as embedded cations). The model $HAl(OH)_3^-X^+$ (whose structure is shown in Scheme 1) is the simplest molecular cluster mimicking the tetrahedral coordination of Al when acting as a substitutional atom for Si in a zeolite framework. The bond between the trivalent Al atom of the subunit $Al(OH)_3$ and the

10.1021/jp982078w CCC: $18.00
Published on Web 05/20/1999

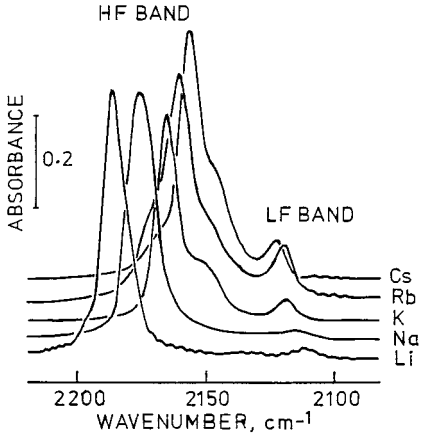

Figure 1. IR results concerning the adsorption of CO at 77 K (nominal) on the set of alkali metal exchanged ZSM-5 zeolites; pressure of about 1 Torr.

oxygen of the zeolite framework is here represented by the H^-, which imparts a formally negative charge to the $HAl(OH)_3^-$ unit; more chemically sound alternatives are either the OH^- or the $OSiH_3^-$ groups. The same reasoning holds for the saturating groups of the $Al(OH)_3$ unit, in which the Si atoms belonging to the zeolite have been represented by H atoms. Results obtained on such a model should, consequently, be taken with some caution. All features found with naked cations have been observed, though understandably to a less marked extent. Again, in that paper the possibility of a double coordination of CO through either the O or the C end has been considered; an ultimate scrutiny of the relevant evidence is, however, lacking.

The present paper discusses the two models envisaged to explain the occurrence of low-frequency IR bands for CO molecules coordinated to cations, namely, (i) simultaneous coordination to two cations and (ii) equilibrium between CO molecules C-bonded and O-bonded to the same cation. Computational results, both previously published[6,10] and carried out for the present purpose, are compared with experimental findings on alkali-exchanged ZSM-5 zeolites, these being the zeolites with the lowest Al/Si ratio and thus providing the simplest examples.

Experimental evidence is also given that the same phenomenon occurs in H-ZSM5. No comparison is, however, carried out with computational data concerning the interaction of a proton with CO, because this is not an appropriate reference. Protonation occurs at either side, yielding the molecular species HCO^+ and COH^+, respectively, with a definitely covalent nature.[11] More appropriate reference is given by the computational results concerning the interaction of CO with cluster models for the Bransted site in zeolites;[12,13] this constitutes, however, a different theme to be developed elsewhere.

2. Survey of Experimental IR Results on Alkali Metal Exchanged ZSM-5 Zeolites

IR spectra illustrating the interaction of CO with the whole set of ZSM-5 zeolites are reported in Figures 1 and 2. Samples employed had a Si/Al ratio equal to 14. The parent Na sample, which was prepared following standard methods,[14] was exchanged with aqueous solutions of the corresponding alkali metal nitrates or with ammonium nitrate to obtain, after thermal treatment, the protonic form of the zeolite. The exchange was complete for NH_4^+ and K^+, about 90%, for Rb^+ and Cs^+, and some 50% for Li^+.

IR spectra of CO adsorbed at liquid nitrogen temperature were obtained following standard methods described elsewhere.[7] The

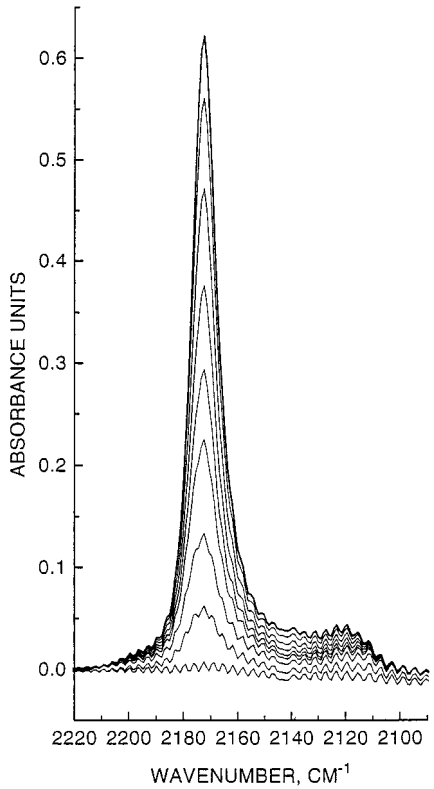

Figure 2. IR spectra of CO adsorbed on H-ZSM-5 zeolite at temperatures ranging from 77 K (nominal, upper spectrum) to room temperature (lower spectrum).

zeolite samples, in the form of self-supporting wafers, were activated at 723 K for 2 h in vacuo prior to dosing with approximately 1 Torr of CO (equilibrium pressure); results corresponding to different CO doses were already reported.[7] Figure 1 shows the results obtained for the alkali metal exchanged zeolites. A main band is always observed at a wavenumber higher than 2143 cm^{-1} (HF species), which, for very low CO equilibrium pressure, was found to peak at 2188, 2178, 2166, 2162, and 2157 cm^{-1} for LiZSM-5 to CsZSM-5, respectively.[7] This cation-specific HF band was assigned to the fundamental C−O stretching mode of carbon monoxide interacting through the C end with the corresponding metal ion; this interaction is essentially electrostatic in nature, since a linear dependence was found[7] between the C−O stretching frequency and the parameter $1/(R_M + R_{CO})^2$, where R_M is the cation radius. Minor shoulders present on the main band are due either to the simultaneous presence of Na^+ (in zeolites not completely exchanged) or to slightly different cation environments; these effects will not be discussed here since they do not affect the subject of the paper. Figure 1 also shows that all spectra display a weak band below 2143 cm^{-1} (LF species), the exact frequency of which is given in Table 1. Note that, along the Li^+ to Cs^+ series, the frequency of HF species decreases, whereas that of LF species increases. The relative intensity A_{HF}/A_{LF} also markedly decreases from Li^+ to Cs^+. For reasons that follow, the LF band is assigned to CO interacting through the oxygen end with cations.

Figure 2 shows the spectra of CO adsorbed at liquid nitrogen temperature (top spectrum) on HZSM-5 and the effect of gradually increasing the temperature of the (closed) IR cell. This was done by allowing the cooling liquid nitrogen bath to evaporate; the last (bottom) spectrum was taken at room temperature, but we could not measure the temperatures corresponding to the intermediate spectra. Again, a main band

TABLE 1: Experimental IR Data for Alkali-Substituted ZSM-5, Derived Thermodynamic Quantities, and Comparable Computational Data[a]

system	ν(HF)	ν(LF)	A_{HF}/A_{LF}	K_e	$-\Delta G_r^\circ$	$-\Delta G_r^\circ$(e)	$-\Delta G_r^\circ$(n)
LiZSM-5	2188	2108	57.1	168	1.02	1.23	3.41
NaZSM-5	2178	2113	24.3	61	0.82	1.11	2.61
KZSM-5	2166	2117	7.69	15	0.54	0.49	1.41
RbZSM-5	2162	2119	7.21	13.5	0.52	0.42	1.1
CsZSM-5	2157	2122	6.42	11	0.48	0.35	0.88
HZSM-5	2172	2115					

[a] ν(HF), CO stretching high-frequency band; ν(LF), CO stretching low-frequency band; A_{HF}/A_{LF}, ratio of the intensities of HF to LF bands; K_e and ΔG_r° equilibrium constant and standard change in Gibbs free energy at 77 K of the process $X^+\cdots OC/X^+\cdots CO$; ΔG_r°(e) and ΔG_r°(n) are the B3-LYP standard changes in Gibbs free energy at 77 K for the embedded and naked cations, respectively. Frequencies in cm^{-1}, energetic data in kcal/mol.

TABLE 2: B3-LYP Data Concerning the Interaction of CO with Single Naked Alkaline Cations[10,a]

	ν(CO)	$\nu(X^+\cdots C)$	$\delta(X^+\cdots C)$	A(CO)	BE	$-\Delta H^\circ(0)$
Li^+-CO	2317	365	227	22	16.6	15.2
Na^+-CO	2296	192	178	32	10.5	9.5
K^+-CO	2275	114	136	42	5.8	5.1
Rb^+-CO	2268	85	125	45	4.6	4.0
Cs^+-CO	2261	67	107	48	3.5	3.0
Li^+-OC	2126	381	139	207	12.7	11.8
Na^+-OC	2148	211	115	169	7.6	6.9
K^+-OC	2166	140	96	144	4.3	3.7
Rb^+-OC	2172	86	89	136	3.3	2.9
Cs^+-OC	2178	59	75	128	2.4	2.1

[a] Frequencies in cm^{-1}, BE and $\Delta H^\circ(0)$ in kcal/mol, infrared intensities A in km/mol.

is observed at 2172 cm^{-1} together with a weak feature at about 2115 cm^{-1}. They should correspond to the aforementioned HF and LF bands, respectively. Table 1 shows that the protonic zeolite HZSM-5 also fits the general trend: the wavenumber of the LF band falls between the corresponding values for NaZSM-5 and KZSM-5, and the same applies to the HF band.

3. Computational Methods

In our previous paper[6] concerning the interaction of CO with a single naked alkali metal cation, it has been shown that quite satisfactory results are obtained with the B3-LYP method,[15,16] which turned out to be comparable to the highest quality results QCISD(T). Results for the embedded cations[10] have also been obtained at the same level of computation. In the present paper, therefore, the B3-LYP method has been adopted systematically and new calculations have also been carried out at the same level of treatment. B3-LYP combines a Becke gradient-corrected exchange functional containing a tuned fraction of Hartree−Fock exchange with a gradient-corrected correlation functional due to Lee, Yang, and Parr proposal.

The basis set adopted for Li^+, Na^+, and K^+ ions, as well as for C and O atoms, was the fully optimized triple-ζ valence basis set (TZV) recently proposed by Ahlrichs and co-workers.[17] Contraction schemes were as follows: C and O (62111/411), Li (62111), Na (73211/51), and. K (842111/631). The TZV basis set has also been supplemented by a double set of polarization d functions on C and O atoms ($\zeta d = 0.15/1.0$) (d set consists of five primitive functions) and by adding a double set of diffuse p functions on the cations, i.e., $\zeta_p(Li) = 0.06/0.4$; $\zeta_p(Na) = 0.0196/0.131$; $\zeta_p(K) = 0.015208/0.041737$. Calculations have been carried out all-electron for the three lighter cations, whereas an ab initio effective core potential has been used to replace the innermost core electrons for Rb^+ and Cs^+; the outermost core orbitals, corresponding to the ns^2np^6 configuration, not replaced by the effective core potential, were treated in the same way as the $(n + 1)$s and $(n + 1)$p valence orbitals following the Hay and Wadt "small-core" scheme.[18] The s-valence part has been further decontracted with respect to the original proposal in order to increase flexibility, giving rise to the following contraction schemes: K (4311/311), Rb (4311/321), and Cs (4311/321), respectively. The basis sets have been obtained at the Internet address as described in ref 19.

New calculations for the CO molecule interacting through both ends with a pair of cations have been run. A number of different configurations have been considered, which are gathered in Scheme 1. For all couples of homologous cations, structure *a* has been studied by imposing a set of values for the $X^+\cdots X^+$ distance (X^+ = Li, Na, K, Rb, Cs), and optimizing the $X^+\cdots C$ and the C−O distance keeping an axial structure. Other structures in Scheme 1 have only been dealt with for a couple of Na^+ cations at fixed distances.

Geometry optimization for all types of complexes has been carried out using analytical gradient techniques and imposing axial symmetry when appropriate. Enforcing axial symmetry for structures a and c of Scheme 1 gives optimized structures as true minima. For all other cases, the symmetry constraints were imposed to simulate structures which may become relevant in a real zeolite, where multiple interactions of CO may occur. Basis set superposition error (BSSE) has been evaluated using the full counterpoise method[20] for all structures; the BSSE correction resulted, however, to be rather small in all cases (of the order of ~1 kJ mol^{-1}).

The binding energy, BE, for each adduct was evaluated by subtracting the total energy of the cation(s) and the CO molecule from that of the adduct itself calculated at the same level of treatment. Harmonic normal-mode frequencies were computed by adopting analytical second energy derivatives and solving the equations of nuclear motion by standard methods.[21] All calculations have been carried out using the Gaussian-94 code.[22]

4. Survey of Computational Results on the Interaction of CO with Single Alkali Metal Cations

Data from our previous work[6] are gathered in Table 2, whereas the reader is referred to the original paper as far as the embedded cations are concerned.[10] Ab initio calculations confirm the basically electrostatic nature of the interaction

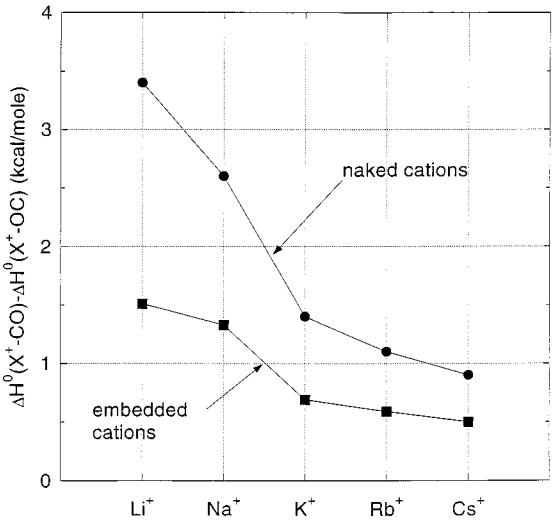

Figure 3. Difference between the standard enthalpies of formation at 0 K of C-bonded adducts, $\Delta H°(X^+-CO)$, and of O-bonded adducts, $\Delta H°(X^+-OC)$, for both naked and cluster embedded alkaline cations. Data (kcal/mol) computed at B3-LYP level.

between CO and alkali metal cations. The reader is however referred to refs 6 and 10 for a rather extensive discussion of the bond. Figure 3 reports the difference between the enthalpy of interaction, at absolute zero, for the whole set of cations both naked and embedded, for C-bonded and O-bonded adducts. The preference for interaction through the C end is evident, as well as the decrease of the energy gap between the two modes of interaction when going from Li^+ to Cs^+. Note also that the enthalpy difference between X^+-CO and X^+-OC adducts is smaller for embedded (as compared to naked) cations.

Figure 4a reports the values of the binding energy BE for both the X^+-CO and X^+-OC adducts (X^+ taken as a naked cation) plotted against the corresponding $\Delta\nu$(CO) values. Figure 4b shows the corresponding data obtained for embedded cations. Note that coordination through the C end imparts a blue shift, and that through the O end a red shift, as expected. A parabolic trend is observed in both cases, which can be accounted for by simple electrostatic considerations.[6] Also worth noting is the slight deviation from the parabolic line for the embedded Li^+-OC adduct; this deviation reflects the well known tendency of Li^+ to engage in partially covalent bonds with the surrounding oxygens.[10]

In our previous papers,[6,10] it has been shown that a direct proportionality is computed between $\Delta\nu$(CO) and the electric field exerted by the cation (either naked or embedded) at the center of mass of the CO molecule, which again suggests that the nature of the interaction is basically electrostatic. This applies to both C-bonded and O-bonded adducts.

Figure 5 reports the specific intensity of the $\nu(C-O)$ mode as a function of the frequency shift, $\Delta\nu(C-O)$. O-bonded complexes are to the left (red shift), and C-bonded complexes to the right (blue shift). The corresponding value for the unperturbed CO molecule is also reported. With naked cations, a nearly linear trend is observed though with different slope at either side. Intensities decrease for increasing values of $\Delta\nu$ in the C-bonded adducts, and the opposite applies to O-bonded species; this feature is accounted for by electrostatic considerations.[6] With embedded cations, the dependence of the specific intensity on the frequency shift is less marked for C-bonded adducts and more so for O-bonded adducts; we have no ready explanation for this, and none was given in the original paper.[10] Also noticeable are the deviations from the linear trend observed

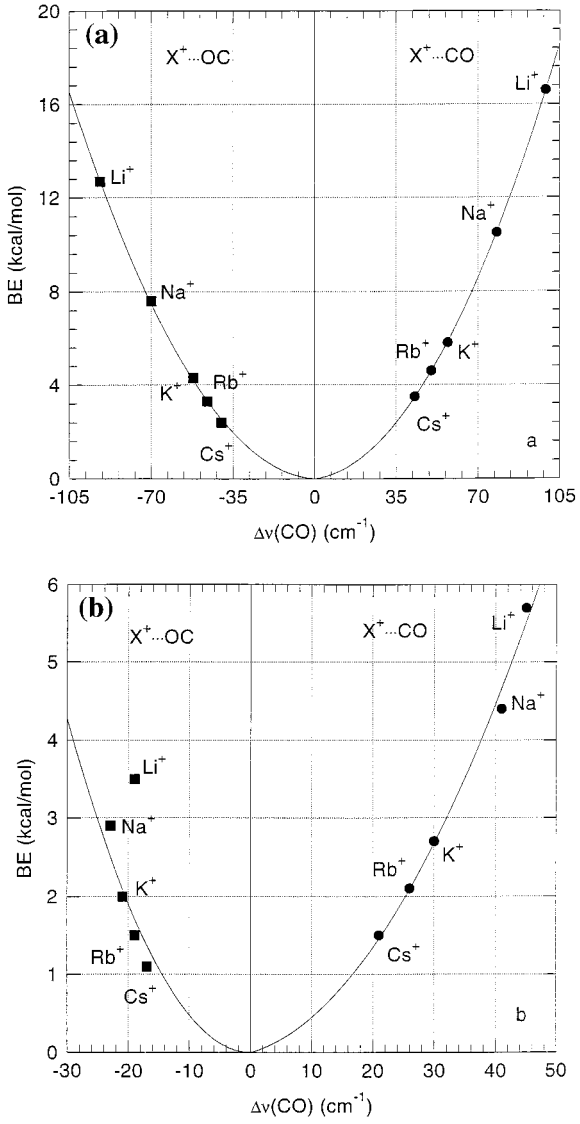

Figure 4. B3-LYP binding energies BE (kcal/mol) versus the corresponding $\Delta\nu$(CO) values (cm^{-1}): (a) naked cations; (b) cluster-embedded alkaline cations.

for the Li^+ cation, again probably ascribable to some covalency in the Li^+-surface oxygen bonds. With O-bonded adducts, even Na^+-OC shows a significant deviation from the main trend.

5. Results on the Interaction with a Pair of Cations

Being that the Si/Al ratio in the adopted ZSM-5 systems is only 14, it is unlikely that couples of adjacent cations are numerous. Judging on the basis of the relative intensities, however, the LF bands appear as minor features so that their connection to exceptional situations, like pairs of cations, cannot be ruled out. Moreover, as it is possible that cations occur at various geometries in the unit cell, we refrained from considering any particular distance between cations on the basis of structural data and chose a set of feasible distances (to be kept fixed during the calculations). We have considered in the first instance a CO molecule aligned with a pair of identical cations (structure a in Scheme 1). As a preliminar investigation, we considered a pair of Cs^+ cations kept separated by a fixed distance of 11 Å, while varying the $Cs^+\cdots C$ distance from 3.2 to 6.8 Å, respectively. For each case, the CO bond distance has been optimized. The binding energy as a function of such a distance is reported in Figure 6. Two minima in the curve are

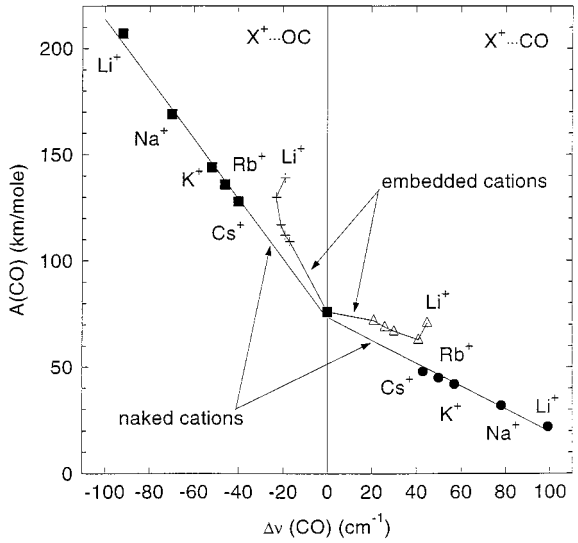

Figure 5. Correlation between B3-LYP infrared intensity of the ν(CO) mode (km/mol) with the corresponding shift $\Delta\nu$(CO) (cm^{-1}) for the CO interacting with naked and embedded cations. O-bonded complexes to the left side (red shift), and C-bonded complexes to the right side (blue shift).

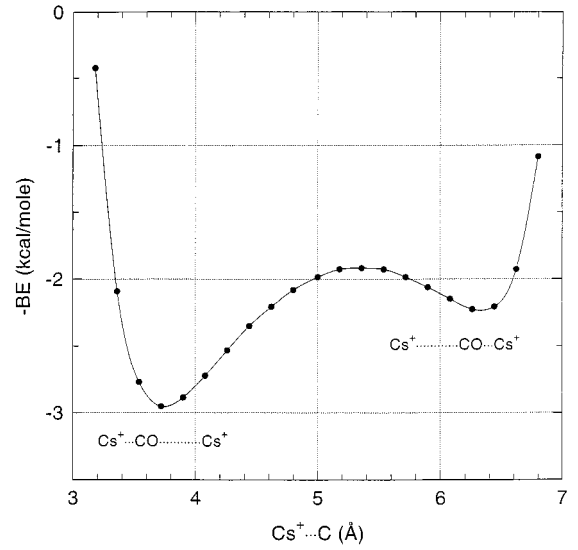

Figure 6. Carbon monoxide interacting at both ends with two Cs^+ cations separated by 11 Å. B3-LYP binding energy BE values (kcal/mol) as a function of the $Cs^+\cdots C$ atom distance.

clearly seen, corresponding to the stable configurations C-bonded and O-bonded, respectively, somewhat perturbed by the presence of the other cation. At both minima, the computation of the CO stretching frequency is possible. However, only the most stable C-bonded configuration has been considered.

A similar result was found for other couples of identical cations and for other distances. Table 3 gathers the results of the calculations for all types of cation couples, whose cation−cation distance was kept fixed at 5, 7, 9, and 11 Å, respectively, together with the case of infinite separation between cations corresponding to CO interacting with a single bare cation.

The most evident result is that the presence of a second cation destabilizes the adduct. In all cases, the interaction energy of the adduct without the second cation is higher; at short distances, the adduct even becomes unbound (negative values in Table 3). This feature can be understood qualitatively on the basis of the electrostatic model of interaction; the electric field at the center of mass of the CO molecule exerted by the two cations, being the algebraic sum of the two electric fields exerted by each, is bound to be smaller than the single cation contribution.

TABLE 3: B3-LYP Data Concerning the Interaction of CO with Two Alkaline Cations at Various Distances[a]

	$R = 5$	$R = 7$	$R = 9$	$R = 11$	$R = \infty$
BE	13.6	14.0	14.7	15.4	16.6
$Li^+\cdots C$	2.036	2.203	2.185	2.183	2.183
ν(CO)	2328	2298	2309	2312	2317
A(CO)	100	44	31	27	22
$\Delta\nu$(CO)	110	80	91	94	99
BE	−19.0	9.1	9.0	9.5	10.5
$Na^+\cdots C$	2.017	2.657	2.572	2.566	2.562
ν(CO)	2499	2260	2285	2290	2296
A(CO)	99	69	44	38	32
$\Delta\nu$(CO)	281	42	67	72	78
BE	−123.8	3.7	3.2	3.3	5.8
$K^+\cdots C$	2.014	3.046	3.164	3.131	3.118
ν(CO)	2852	2247	2256	2266	2275
A(CO)	124	93	61	51	42
$\Delta\nu$(CO)	634	29	38	48	57
BE	−223.2	1.4	4.0	3.9	4.6
$Rb^+\cdots C$	2.016	3.047	3.473	3.391	3.368
ν(CO)	3168	2266	2244	2257	2268
A(CO)	136	97	69	55	45
$\Delta\nu$(CO)	950	48	26	39	50
BE	−377.3	−7.0	3.4	3.0	3.5
$Cs^+\cdots C$	2.023	3.043	3.874	3.739	3.683
ν(CO)	3517	2296	2231	2248	2261
A(CO)	190	108	81	61	48
$\Delta\nu$(CO)	1299	78	13	30	43

[a] R is the cation−cation separation; $R = \infty$ refers to a single naked cation interacting with CO; $X^+\cdots C$ is the cation−carbon distance of the optimized structure. Frequencies in cm^{-1}, binding energy BE in kcal/mol, distances in Å. The calculated reference value for the stretching frequency of gaseous CO is 2218 cm^{-1}.

The C−O stretching frequency, however, always higher than the gas-phase value; the blue shift in the CO frequency imparted by the cation at the C side is never compensated by the red shift caused by that at the O side.

At very short distances of the two cations, repulsion between the C and 0 atoms and the cations yields artificially high values of ν(CO) together with negative binding energies. The relationship between BE and $\Delta\nu$(CO) is illustrated in Figure 7 for all cations at selected cation−cation distances. Points falling to the parabolic dashed curve are for infinite cation−cation distance, i.e., the CO interacts with a single bare cation; the dependence between BE and $\Delta\nu$(CO) is the same as that already shown in the rightmost part of Figure 4a. However, for CO interacting with a given pair of cations, the points relative to different cation−cation separation are aligned on a parabola (continuous lines in Figure 7) with definite minima so that the proportionality between BE and $\Delta\nu$(CO) no longer holds.

In conclusion, axial interaction with a pair of cations (as in structure a) is not able to explain experimental ν(CO) values lower than 2143 cm^{-1}. Since when the two cations are close to each other the CO molecule cannot interact axially with them and indeed the system is unbound, other configurations may be possible. Some of them are gathered 9 in Scheme 1; concerning these, although ab initio calculations have been carried out in detail, only qualitative features are reported for the sake of brevity. Structures having the C−O axis parallel to the cation−cation direction (structure a′) do not correspond to energy minima. This is also the case for the structure (denoted as a″ in Scheme 1) envisaging the end-on interaction with one cation (via the C end) and side-on interaction with the other.

Considering perpendicular arrangements of the CO molecule

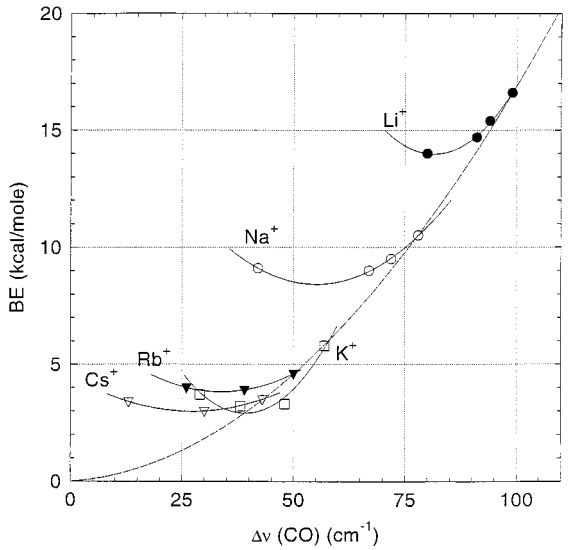

Figure 7. Correlation between the B3-LYP $\Delta\nu$(CO)(cm^{-1}) and the BE (kcal/mol) for the X$^+$···CO···X$^+$ linear systems. Points on each continuous line refer to different X$^+$···X$^+$ distances. The leftmost point corresponds to the shortest X$^+$···X$^+$ distance. Points on the dashed parabola are for infinite X$^+$···X$^+$ separation (single bare cation).

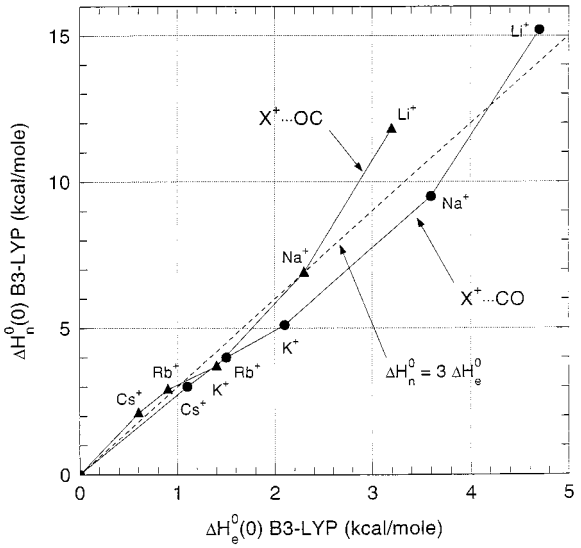

Figure 8. Correlation between computed B3-LYP heats of formation for C-bonded and O-bonded adducts for naked cations (ΔH°_n) with respect to embedded ones (ΔH°_e). Data in kcal/mol.

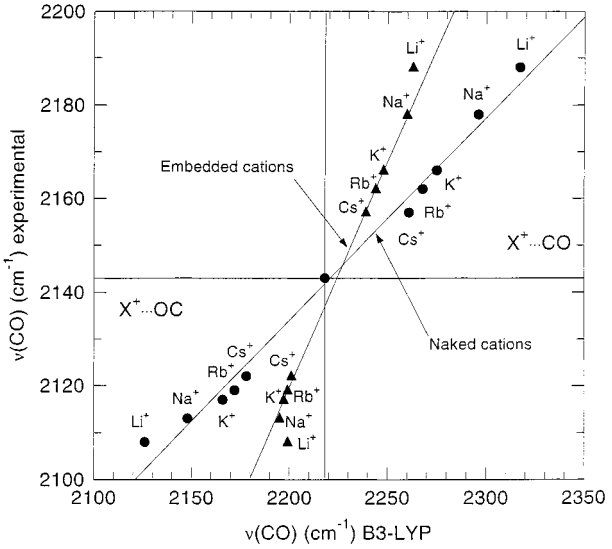

Figure 9. Correlation between the experimental and B3-LYP computed values of ν(CO) (cm^{-1}) for both naked and embedded cations: (upper) HF bands; (lower) LF bands.

with respect to the cation−cation axis, two situations are met. At short X$^+$···X$^+$ distances (structure b in Scheme 1) a minimum-energy configuration was found, with CO symmetrically lying between the two cations, which act basically as a single cation with a larger effective positive charge. At large X$^+$···X$^+$ distances, structure b becomes unstable and structure b′ has been therefore investigated. This resulted, however, to be unstable and evolves to structure c, in which the CO molecule is, aligned axially with the, cations, but lies outside. All these findings may readily be rationalized in terms of electrostatics.

These results, though useless to the present purpose of explaining LF bands, may however help in understanding the adsorption of CO in basic zeolites with high Al content (X and Y), where IR bands, corresponding to relatively strong interactions, were found in the neighborhood of 2143 cm^{-1}.[23]

6. Comparison between Computational Results and Experiment

When directly comparing experimental data on ZSM-5 systems with computational results for naked cations, the role of the zeolite framework is being neglected. However, framework effects are far from being negligible. For instance, whereas with mordenite or ZSM-5, CO interaction takes place only at low temperature (and is typically studied at 77 K), with Na−Y, interaction takes place already at room temperature. This has allowed the direct calorimetric evaluation of the interaction enthalpy.[2]

Results on embedded cations[10] confirm the role of framework oxygen atoms in modulating the features of cation−CO interaction. Figure 8 shows the correlation between $\Delta H^\circ(0)$ values computed for naked and embedded cations. It is worth noting that the zeolite framework, simulated by the $Al(OH)_3H^-$ cluster, reduces all $\Delta H^\circ(0)$ values computed for the naked cations to about 1/3 (dashed straight line). Such a correlation is strictly followed in the case of X$^+$−OC complexes for Cs$^+$, Rb$^+$, K$^+$, and Na$^+$ cations, whereas a significant deviation is seen for the Li$^+$ cation, here again because covalency is coming into play in the bond between Li$^+$ and the oxygen atoms of the $Al(OH)_3H^-$ cluster, which reduces the effective electric field created by the Li$^+$ ion. Similar arguments also hold for the X$^+$−CO case.

Two experimental values are available for the energy of interaction of CO with Na-exchanged zeolite Y, i.e., 6.7[2] and 8.4 kcal/mol.[24] The B3-LYP $\Delta H^\circ(0)$ value for naked cations is 9.5 kcal/mol, in obvious excess with respect to the experiment. The value of 3.6 kcal/mol computed for the embedded cations is instead definitely underestimated. The reason is probably the same one outlined above, i.e., the embedding cluster $Al(OH)_3H^+$ has too strong interactions with the Na$^+$ ion, which in turn, interacts too weakly with the CO molecule.

The upper part of Figure 9 shows the comparison of the $\Delta\nu$(CO) shifts measured for the whole set of alkali metal exchanged ZSM-5 zeolites (Table 1) with the results of B3-LYP calculations (Table 2), for both naked and embedded cations. A good proportionality is seen for the naked cations case, whereas deviation from a simple linear behavior is seen for the case of embedded cations when the Li$^+$ ion is considered. However, the presence of the cluster brings the computed

ν(CO) values in better agreement with those measured on cation-exchanged ZSM-5. In the case of Na−Y, for example, the calculated values of $\Delta\nu$(CO) are 78 and 42 cm^{-1} for the naked cations and embedded clusters, respectively, to be compared with the experimental value of 26 cm^{-1}.[2]

In conclusion, calculated values for the interaction of CO with naked cations can be used as a guide for interpreting the adsorption of CO on alkali metal exchanged zeolites, notwithstanding the absence of surrounding oxygen anions, because of which the interaction tends to be significantly more marked. On the other hand, embedded cations yield more mitigated values, but overestimation of covalency between the cation and framework oxygen atoms may lead to spurious effects.

7. Equilibrium between C-Bonded and O-Bonded Adducts

The comparison between calculated frequencies for O-bonded adducts with the naked cations (Table 2) and measured LF bands (Table 1) is made in the lower part of Figure 9. As is the case with the high-frequency bands (upper part of Figure 9), there is a neat, almost linear correlation between the two types of data. Shifts are also in this case much larger for computed values than for experimental ones, for the same reasons holding for the high-frequency bands. Both curves for C-bonded and O-bonded adducts pass through the origin, which is given by the data corresponding to the isolated CO molecule: 2143 cm^{-1} (experimental data) and 2218 cm^{-1} (value computed at B3-LYP level). The two sets of data seem actually to merge into the same curve. Figure 9 also reports similar data for embedded cations, for which similar considerations hold. A straight line passes through most data, the reference value for CO in the absence of cations being different from the previous one. These spectroscopic features lend support to the coexistence of C-bonded and O-bonded adducts: further evidence comes from thermodynamic considerations.

In the hypothesis that LF bands are due to CO molecules O-bonded to the same sites giving rise to the HF bands, one may write an isomerisation process

$$X^+\cdots OC \rightleftharpoons X^+\cdots CO \qquad (1)$$

the standard free-energy change of which is denoted hereafter by ΔG_r°. It is evident from inspection of Figure 1 that on going from Li^+ to Cs^+ the relative weight of the low-frequency band increases; i.e., the equilibrium constant K_e of (1) decreases in the same direction. This is in qualitative agreement with the fact that, along the same series, the enthalpy of formation of C-bonded and of O-bonded adducts approach one another. To put this concept on a quantitative basis, the following procedure has been followed. The intensity ratio between the high-frequency band and the low-frequency one has been measured in each case. To take into account that, upon adduct formation, the specific intensity of the CO stretch varies (more specifically, that of C-bonded adducts decreases and that of O-bonded adducts increases), we have made use of the relationship established computationally (Figure 5) between the specific infrared intensity and the shift in CO frequency, applied to the experimental values. This yielded reasonable values for the specific intensities of each band, from which K_e values, and the corresponding ΔG_r° values listed in Table 1 were calculated.

For the computational side, the calculation of the corresponding ΔG_r°(e) and ΔG_r°(n), respectively, for the embedded and naked cations, is straigthforward from the knowledge of both structures and vibrational frequencies, which allows the calculation of the enthalpic and entropic corrections to the binding energy to be estimated by means of the classical statistical formulae computed at 77 K (see Table 1).

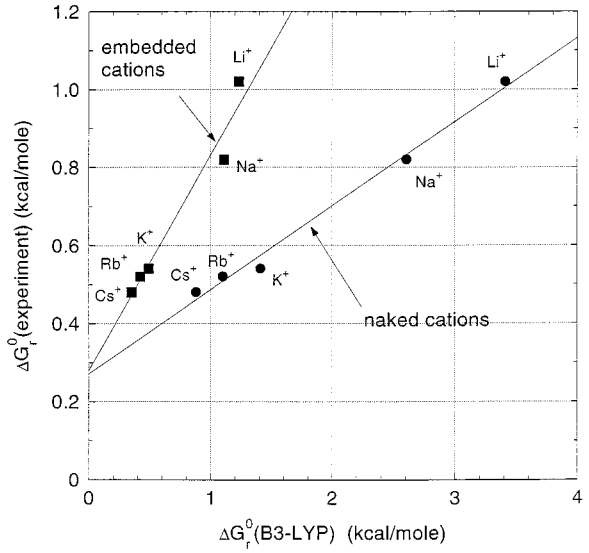

Figure 10. Correlation between the experimental estimate of ΔG_r° (kcal/mol) and the corresponding B3-LYP ΔG_r° values for the interaction with both naked and embedded cations.

Both these sets of results are plotted in Figure 10. The experimental values and the computational ones show an excellent linear correlation. The plots do not pass, however, through the origin. A vanishing computed value of ΔG_r° corresponds to the absence of any interaction with cations; the observed nonvanishing intercept must therefore correspond to the effect of the zeolite matrix, deprived of cations. This is apparently not accounted for with the cluster model, as a similar intercept is observed as with bare cations. The zeolite matrix makes a positive contribution to ΔG_r° of some 1.2 kJ/mol. This corresponds to a destabilization of O-bonded adducts with respect to C-bonded adducts.

8. Concluding Remarks and Outlook

In our previous paper,[6] the conclusion was drawn that, although adducts formed by CO with naked cations represent only a crude model for the interaction of the same molecule with alkali metal substituted zeolites, calculations performed on these models were able to account for the main features experimentally observed for CO/zeolite systems: formation of stable species, heats of formation, magnitude of the shift in the CO stretching frequency, and decreasing trend of the CO intensity with increasing strength of interaction. However, because of the destabilizing role of the oxygen atoms surrounding the cation in the zeolitic systems, all calculated quantities are in excess with respect to the real systems. Adopting a minimal-size cluster model embedding the cation[10] reduces indeed to about one-third of the interaction energies. A spurious covalency, however, between the lightest cations and the surrounding oxygen atoms is introduced by the limited size of the model.

The use of the same set of data, concerning this time also O-bonded adducts of CO with naked cations, allowed us to accumulate sufficient evidence that binding of CO through the O end does take place in basic zeolites, as suggested by Katoh et al.[9] This is so because of the proximity of the corresponding energy levels, i.e. by an equilibrium distribution between two close-lying energy states. The hypothesis involving double

coordination of CO to two cations, either in a linear configuration or involving side-on interactions, can be discarded on the basis of the present calculations.

We also remark that the protonic HZSM-5 zeolite shows the same general features as cation-exchanged zeolites, that is, both a HF and a LF band have been observed, which suggests an equilibrium between C-bonded and O-bonded CO adducts.

The present results deserve some comment, because they represent, to the best of our knowledge, the first well-documented case of O-bonded carbon monoxide as far as both Lewis and Brönsted sites are concerned. The intriguing question is why O-bonded CO adducts were not observed on metal oxides or halides, the immense literature on the subject notwithstanding. We are aware of the fact that a satisfactory answer will require much work, especially computational, to shed light on a different matter.

A possible key factor lies in the fact that cations in a zeolite are much more protruding than those at the surface of metal oxides and halides, thus being closer to the situation of the naked ion. Indeed, the heats of adsorption on cation-echanged Y zeolites (e.g., Na and Zn) are higher than the heats of adsorption on the corresponding halides and oxides.[2,24] On the surface of a bulk solid, like NaCl, cations are in a higher coordination state, and the surrounding anions (oxygen or halide ions) surely destabilize to a larger extent both C-bonded and O-bonded adducts.

Figure 10, moreover, seems to suggest that the anions surrounding the cation destabilize the O-bonded adducts to a larger extent. As a consequence, the energy gap between C-bonded and O-bonded adducts widens and the latter state is not populated.

A possible explanation for these effects is that the 5σ orbital of the CO molecule (localized mainly on the C atom) has a strong p character and is directed along the axis of the molecule; by contrast, the 3σ orbital, mainly localized on the O atom, has a more pronounced s character, i.e., it is less directional. Anions surrounding a cation are therefore more likely to suffer repulsion from the O end than from the C end of the molecule.

Finally, we suggest that perhaps O-bonded adducts could be observed for CO adsorbed on metal oxides having a high proportion of highly coordinatively unsaturated cations. This situation could arise when considering very highly divided materials, where cations at corners of small crystals could represent a significant proportion of the surface-exposed metal ions.

References and Notes

(1) Seanor, D. A.; Amberg, C. H. *J. Chem. Phys.* **1965**, *42*, 2967.

(2) Bolis, V.; Fubini, B.; Garrone, E.; Giamello, E.; Morterra, C. In *Structure and Reactivity of Surfaces*; Morterra, C., et al., Eds.; Elsevier: Amsterdam, 1989; p 159.

(3) Pisani, C. *J. Mol. Catal.* **1993**, *82*, 229.

(4) Pacchioni, G.; Cogliandro, G.; Bagus, P. S. *Surf. Sci.* **1991**, *255*, 344.

(5) Neyman, K. M.; Ruzankin, S. Ph.; Rösch, N. *Chem. Phys. Lett.* **1995**, *246*, 546.

(6) Ferrari, A. M.; Ugliengo, P.; Garrone, E. *J. Chem. Phys.* **1996**, *105*, 4129.

(7) Zecchina, A.; Bordiga, S.; Lamberti, C.; Spoto, G.; Carnelli, L.; Otero Areán, C. *J. Phys. Chem.* **1994**, *98*, 9577.

(8) Bordiga, S.; Lamberti, C.; Geobaldo, F.; Zecchina, A.; Turnes Palomino, G.; Otero Areán, C. *Langmuir* **1995**, *11*, 527.

(9) Katoh, M.; Yamazaki, T.; Ozawa, S. *Bull. Chem. Soc. Jpn.* **1994**, 67, 1246.

(10) Ferrari, A. M.; Neyman, K. M.; Roesch, N. *J. Phys. Chem. B* **1997**, *101*, 9292.

(11) Nobes, R. H.; Radom, L. *Chem. Phys.* **1981**, *60*, 1.

(12) Senchenya, I. N.; Garrone, E.; Ugliengo, P. *J. Mol. Struct. (THEOCHEM)* **1997**, *368*, 93.

(13) Civalleri, B.; Garrone, E.; Ugliengo, P. *J. Phys. Chem. B* **1998**, *102*, 2373.

(14) Szostak, R. In *Molecular Sieves*; van Nostrand Reinhold: New York, 1989.

(15) Becke, A. D. *J. Chem. Phys.* **1993**, *98*, 5648.

(16) Lee, C.; Yang, W.; Parr, R. G. *Phys. Rev.* **1988**, *B37*, 785.

(17) Schafer, A.; Huber, C.; Ahlrichs, R. *J. Chem. Phys* **1994**, *100*, 5829.

(18) Hay, P. J.; Wadt, W. R. *J. Chem. Phys.* **1995**, *82*, 299.

(19) Basis sets were obtained from the Extensible Computational Chemistry Environment Basis Set Database, version 1.0, as developed and distributed by the Molecular Science Computing Facility, Environmental and Molecular Sciences Laboratory, which is part of the Pacific Northwest Laboratory, P.O. Box 999, Richland, WA 99352, and funded by the U. S. Department of Energy. The Pacific Northwest Laboratory is a multiprogram laboratory operated by Battelle Memorial Institue for the U. S. Department of Energy under Contract DE-AC06-76RLO 1830. Contact David Feller, Karen Schuchardt, or Don Jones for further information.

(20) Boys, S. F.; Bernardi, F. *Mol. Phys.* **1970**, *19*, 553.

(21) Wilson, E. B.; Decius, J. C.; Cross, P. C. *Molecular Vibrations*; McGraw-Hill: New York 1955.

(22) Frisch, M. J.; Trucks, G. W.; Schlegel, H. B.; Gill, P. M. W.; Johnson, B. G.; Robb, M. A.; Cheeseman, J. R.; Keith, T.; Petersson, G. A.; Montgomery, J. A.; Raghavachari, K.; Al-Laham, M. A.; Zakrzewski, V. G.; Ortiz, J. V.; Foresman, J. B.; Cioslowski, J.; Stefanov, B. B.; Nanayakkara, A.; Challacombe, M.; Peng, C. Y.; Ayala, P. Y.; Chen, W.; Wong, M. W.; Andres, J. L.; Replogle, E. S.; Gomperts, R.; Martin, R. L.; Fox, D. J.; Binkley, J. S.; Defrees, D. J.; Baker, J.; Stewart, J. P.; Head-Gordon, M.; Gonzalez, C.; Pople, J. A. *Gaussian 94*, revision C.3; Gaussian, Inc.: Pittsburgh PA, 1995.

(23) Garrone, E.; Zecchina, A.; Otero Areán, C. Unpublished.

(24) Kuroda, Y.; Yoshikawa, Y.; Kumashiro, R.; Nagao, M. *J. Phys. Chem. B* **1997**, *101*, 6497.